

On Revealing the Hidden Problem Structure in Real-World and Theoretical Problems Using Walsh Coefficient Influence

Michał W. Przewozniczek
Wrocław Univ. of Science and Techn.
Wrocław, Poland
michal.przewozniczek@pwr.edu.pl

Francisco Chicano
ITIS Software, University of Málaga
Málaga, Spain
chicano@uma.es

Renato Tinós
University of São Paulo
Ribeirão Preto, Brazil
rtinos@ffclrp.usp.br

Jakub Nalepa
Silesian Univ. of Technology/KP Labs
Gliwice, Poland
jakub.nalepa@polsl.pl

Bogdan Ruszczak
Opole Univ. of Technology/KP Labs
Opole, Poland
b.ruszczak@po.edu.pl

Agata M. Wijata
Silesian Univ. of Technology/KP Labs
Gliwice, Poland
agata.wijata@polsl.pl

Abstract

Gray-box optimization employs Walsh decomposition to obtain non-linear variable dependencies and utilize them to propose masks of variables that have a joint non-linear influence on fitness value. These masks significantly improve the effectiveness of variation operators. In some problems, all variables are non-linearly dependent, making the aforementioned masks useless. We analyze the features of the real-world instances of such problems and show that many of their dependencies may have noise-like origins. Such noise-caused dependencies are irrelevant to the optimization process and can be ignored. To identify them, we propose extending the use of Walsh decomposition by measuring variable dependency strength that allows the construction of the weighted dynamic Variable Interaction Graph (wdVIG). wdVIGs adjust the dependency strength to mixed individuals. They allow the filtering of irrelevant dependencies and re-enable using dependency-based masks by variation operators. We verify the wdVIG potential on a large benchmark suite. For problems with noise, the wdVIG masks can improve the optimizer's effectiveness. If all dependencies are relevant for the optimization, i.e., the problem is not noised, the influence of wdVIG masks is similar to that of state-of-the-art structures of this kind.

CCS Concepts

• **Mathematics of computing** → **Combinatorial optimization**;
• **Theory of computation** → **Random search heuristics**; • **Computing methodologies** → **Artificial intelligence**.

Keywords

Variable dependency, Gray-box optimization, Genetic Algorithms, Dependency strength, Optimization, Walsh decomposition

ACM Reference Format:

Michał W. Przewozniczek, Francisco Chicano, Renato Tinós, Jakub Nalepa, Bogdan Ruszczak, and Agata M. Wijata. 2025. On Revealing the Hidden Problem Structure in Real-World and Theoretical Problems Using Walsh Coefficient Influence. In *Genetic and Evolutionary Computation Conference*

(GECCO '25), July 14–18, 2025, Malaga, Spain. ACM, New York, NY, USA, 9 pages. <https://doi.org/10.1145/3712256.3726410>

1 Introduction

Gray-box optimization and model-building optimizers in black-box optimization use the knowledge about variable dependencies to improve their performance. Two variables may be considered dependent if their joint influence on the optimized function is non-linear. Such variables shall be processed together by an optimizer. Therefore, dependencies are employed to construct variation masks [26], e.g., for individual mixing [24] or perturbation [23].

To create a high-quality mask, we consider the *problem structure*, i.e., the graph of variable dependencies, to join dependent variables into one cluster. Such mechanisms are effective when dealing with a *strong problem structure* (when the percentage of dependent variable pairs is low). However, if the structure is *weak* (all or almost all variable pairs are dependent), we mainly obtain full masks joining all or almost all variables, which may be useless. To overcome this difficulty, we can estimate the dependency strength to use only the strongest dependencies [22]. However, it may be hard to decide what threshold shall we use for the mask creation.

Walsh decomposition [7, 26, 28] is frequently used in gray-box optimization to discover variable dependencies before the optimization process. To the best of our knowledge, it has only been employed to differentiate dependent from non-dependent variable pairs. Therefore, we extend the usability of Walsh decomposition by obtaining the dependency strength. To this end, we propose, analyze, and experimentally verify different propositions of Walsh-based dependency strength estimation, including the mechanisms that adjust the dependency strength to mixed individuals. Finally, we integrate all these mechanisms in an optimizer that outperforms other state-of-the-art propositions.

To improve the understanding of the applicability of our propositions, we thoroughly investigate the structure-related features of toy-sized instances of several real-world problems arising in the field of Machine Learning. We discover that many dependencies may have noise-like origins and have negligible influence on the optimized function value. As such, these existing dependencies can be ignored while constructing variation masks. These observations show that proposing accurate dependency strength measurement may be a game-changer in the optimization of many real-world problems to which gray-box mechanisms can not be applied today.



This work is licensed under a Creative Commons Attribution 4.0 International License. *GECCO '25, Malaga, Spain*

© 2025 Copyright held by the owner/author(s).
ACM ISBN 979-8-4007-1465-8/2025/07
<https://doi.org/10.1145/3712256.3726410>

Moreover, in optimization, it is frequent to consider non-linear dependencies. Our results show that other dependency types can be significantly more convenient in filtering irrelevant dependencies and obtaining high-quality variation masks.

2 Background

2.1 Gray-box optimization and Walsh decomposition

Gray-box optimization utilizes the knowledge about variable dependencies to leverage the optimization process [26]. It frequently focuses on the k -bounded problems, which can be represented as the sum of subfunctions taking no more than k arguments [27]. The *additive form* is convenient for representing such problems: $f(\mathbf{x}) = \sum_{S=1}^S f_S(\mathbf{x}_{I_S})$, where $\mathbf{x} = (x_1, x_2, \dots, x_n)$ is a binary vector of size n , I_S are subsets of $\{1, \dots, n\}$ (I_S do not have to be disjoint), and S is the number of these subsets.

Walsh decomposition [7] is useful in decomposing k -bounded problems and represent them in as: $f(\mathbf{x}) = \sum_{i=0}^{2^n-1} w_i \varphi_i(\mathbf{x})$, where $w_i \in \mathbb{R}$ is the i th Walsh coefficient, $\varphi_i(\mathbf{x}) = (-1)^{\mathbf{i}^T \mathbf{x}}$ defines a sign, and $\mathbf{i} \in \{0, 1\}^n$ is the binary representation of index i .

Any pseudo-boolean function can be represented using Walsh coefficients. Each coefficient is associated with a mask that marks variables. If at least one mask marks a given pair of variables, then they are non-linearly dependent. Using Walsh coefficients, we can compute a function value for any solution. To this end, we must compute signs of Walsh coefficients by summarizing the binary values of variables marked by a given mask. If the sum is even, then the Walsh coefficient is added or subtracted otherwise. For instance, for a 3-bit function represented by two Walsh coefficients $w_{111} = -5$ and $w_{001} = 2$, the function value for solution 101 will be: $w_{111} - w_{001} = -5 - 2 = -7$.

Consider $f_{px}(x_1, \dots, x_4) = xor(x_1, x_2) + xor(x_2, x_3) + xor(x_3, x_4)$. Note that xor introduces non-linear dependencies between variables. Thus, Walsh decomposition will identify pairs (x_1, x_2) , (x_2, x_3) , and (x_3, x_4) as dependent. The above representation is the additive form of f_{px} , in which subfunctions (each xor) share variables, i.e., overlap. If subfunctions overlap, the function may be hard to optimize because by modifying a shared variable, we modify the output of more than one subfunction at a time. Information about variable dependencies is stored in the Variable Interaction Graph (VIG), which can be represented by a square matrix denoting whether a given pair of variables is dependent or not. VIG for f_{px} is presented in Table S-III (supplementary material). Using VIG, we can propose masks that improve the performance of variation operators. Partition crossover (PX) [24] is a VIG-based mixing operator. For two individuals, it removes all VIG entries that refer to variables equal in mixed individuals and clusters variables based on the remaining ones. For individuals $\mathbf{x}_{p1} = 1110$ and $\mathbf{x}_{p2} = 0011$ it will create two mixing masks $m_{px1} = \{1, 2\}$ and $m_{px2} = \{4\}$. An important feature of PX is that even if subfunctions overlap, it creates masks that allow exchanging subfunction arguments without breaking them, i.e., all the subfunction argument sets in the offspring will be the same as in one of the parents. If we choose m_{px1} and copy genes from \mathbf{x}_{p2} to \mathbf{x}_{p1} , then we will receive $\mathbf{x}_{p3} = 0010$ (first xor has the same arguments as \mathbf{x}_{p1} , second is the same for both parents,

third is the same as in \mathbf{x}_{p2}). Therefore, PX is useful in optimizing overlapping problems [16]. However, if the epistasis of a VIG is high, i.e., all or almost all variables are considered dependent, then PX may create a single mask marking all differing genes. Since such mask is useless, identifying and ignoring dependencies irrelevant to the optimization process can increase effectiveness [3].

2.2 Linkage trees and SLL-using optimizers

In black-box optimization, variable dependencies can be discovered. Statistical Linkage Learning (SLL) [6, 8, 21] predicts the eventual dependencies by analyzing the entropy of variable value frequencies that occur in the population. The Dependency Structure Matrix (DSM) stores the predicted dependency strength between variable pairs. In SLL, we do not know which dependencies are true. Therefore, many SLL-using optimizers cluster DSM to create Linkage Trees (LTs). In an LT, leaves refer to single variables. The most dependent nodes (concerning DSM) are joined and form larger clusters. LT root is a full mask and is useless for optimization. However, the other LT nodes can be used as variation masks.

LT-GOMEA is a state-of-the-art SLL-using optimizer [2]. During its run, it creates subpopulations of increasing size. In each iteration of a given subpopulation, LT-GOMEA builds DSM and LT. It uses Optimal Mixing (OM) to mix individuals. OM involves the *source* individual that is being updated, the *donor* individual and a mask. Genes marked by a mask are copied from the donor to the source. If this operation does not decrease the source fitness, its result is preserved or rejected otherwise. During OM, all LT masks are considered, and a different donor is randomly chosen for each mask.

Parameter-less Population Pyramid (P3) uses SLL and OM, but it also introduces a new way of population management [6]. P3 maintains many subpopulations that resemble a pyramid and are called *levels*. In each iteration, P3 creates a new individual (*climber*). First, it is improved using the First Improvement Hillclimber (FIHC). FIHC flips bits in a random order. If a bitflip improves fitness, it is preserved or rejected otherwise. After FIHC, a copy of the climber is added to the first level of the pyramid. Then, the climber is mixed using OM of subsequent pyramid levels. If OM improves it, then an improved climber's copy is added to the next pyramid level (it is created if it does not exist yet). P3 preserves population diversity well and uses a separate LT for each pyramid level. These features make it effective in solving overlapping problems [15].

2.3 Dependency types

If gray-box mechanisms are unavailable, instead of using SLL, we can discover variable dependencies using variable dependency checks. In non-linearity check [10] x_g and x_h are dependent if: $f(\mathbf{x}) + f(\mathbf{x}^{g,h}) \neq f(\mathbf{x}^g) + f(\mathbf{x}^h)$, where \mathbf{x}^g , \mathbf{x}^h , and $\mathbf{x}^{g,h}$ are the individuals obtained from \mathbf{x} by flipping x_g , x_h or both of them.

In some cases, the non-linearity check may discover dependencies that are irrelevant to the optimization process. Such dependencies should be ignored or eliminated because they can deteriorate the quality of variation masks [11]. To this end, the non-monotonicity check can be used [14, 17], which finds x_g and x_h dependent if at least one of the following conditions is true:

- C1. $f(\mathbf{x}) < f(\mathbf{x}^g) \wedge f(\mathbf{x}^h) \geq f(\mathbf{x}^{g,h})$ C4. $f(\mathbf{x}) < f(\mathbf{x}^h) \wedge f(\mathbf{x}^g) \geq f(\mathbf{x}^{g,h})$
 C2. $f(\mathbf{x}) = f(\mathbf{x}^g) \wedge f(\mathbf{x}^h) \neq f(\mathbf{x}^{g,h})$ C5. $f(\mathbf{x}) = f(\mathbf{x}^h) \wedge f(\mathbf{x}^g) \neq f(\mathbf{x}^{g,h})$

C3. $f(x) > f(x^g) \wedge f(x^h) \leq f(x^{g,h})$ C6. $f(x) > f(x^h) \wedge f(x^g) \leq f(x^{g,h})$
 Directional Direct Linkage Discovery (2DLED) [14] reduces irrelevant dependencies by considering non-symmetrical dependencies. Using C1-C6 conditions, it finds x_g dependent on x_h if C1-C3 holds, and x_h dependent on x_g if C4-C6 holds. It can discover symmetrical or non-symmetrical dependency between two variables.

3 PX with Weighted Dynamic VIG

3.1 Intuitions and motivations

Let us consider a 6-bit problem, which Walsh decomposition is built from four coefficients: $w_{110000} = w_{011000} = w_{001100} = w_{111111} = 1$. We wish to mix two individuals:

- $\mathbf{x}_a = [111101] = w_{110000} + w_{011000} + w_{001100} - w_{111111} = 2$
- $\mathbf{x}_b = [100010] = -w_{110000} + w_{011000} + w_{001100} + w_{111111} = 2$

We may say, we wish to pass the positive sign of w_{110000} from \mathbf{x}_a to \mathbf{x}_b or we wish to pass the positive sign of w_{111111} from \mathbf{x}_b to \mathbf{x}_a . However, for the considered problem, the Walsh-based VIG will be a full graph. Thus, any PX mask will mark all genes and will be useless. The question is whether we must cluster all genes together in this case. Below we analyze two available scenarios.

In the first scenario, we wish to improve \mathbf{x}_b . Thus, we have to copy x_2 from \mathbf{x}_a to pass the positive value of w_{110000} , which will change the sign of w_{011000} in the modified \mathbf{x}_b . Therefore, we have to copy x_3 too, which will change the sign of w_{001100} , and, therefore, we have to copy x_4 . Note that that whenever we flip x_2 to modify the sign of w_{011000} , we have to flip one more variable joined with x_2 by the masks of other Walsh coefficients x_2 belongs to. Note that all dependent gene pairs which dependence arise from the masks of size 2 can be considered unbreakable, i.e., if we want to preserve the sign of such Walsh coefficient and flip one of its variables, then we must flip the other variable too.

Copying x_2, x_3 , and x_4 from \mathbf{x}_a to \mathbf{x}_b will create the following solution $\mathbf{x}_b' = [111110]$, in which the value of w_{111111} will be negative. Therefore, after copying x_4 , we have to copy **one** more gene, x_5 or x_6 , i.e., we can choose one of the remaining genes marked by w_{111111} . Thus, we do not have to use a mask that covers all dependencies arising from w_{111111} .

In the second scenario, we wish to improve \mathbf{x}_a by passing the positive value of w_{111111} , but do not modify the genes marked by w_{110000}, w_{011000} , and w_{001100} . Therefore, we have to copy x_5 or x_6 from \mathbf{x}_b to \mathbf{x}_a . Although w_{111111} marks six genes, we must copy only one to pass the positive value of w_{111111} .

The above examples show that gene relations arising from long masks seem much weaker than those arising from short masks. Let us consider an example of a 7-bit problem, which Walsh decomposition is built from four coefficients: $w_{1100000} = w_{0111100} = w_{0000110} = w_{0000011} = 1$. We wish to mix two individuals:

$\mathbf{x}_c = [1110011] = w_{1100000} + w_{0111100} - w_{0000110} + w_{0000011} = 2$
 $\mathbf{x}_d = [0010110] = w_{1100000} + w_{0111100} + w_{0000110} - w_{0000011} = 2$
 We wish to pass the positive value of $w_{0000110}$ from \mathbf{x}_d to \mathbf{x}_c . Therefore, we copy x_5 from \mathbf{x}_d to \mathbf{x}_c , which makes $w_{0111100}$ negative. The mask size of $w_{0111100}$ is 4 but except x_5 the only gene covered by $w_{0111100}$ and differing in \mathbf{x}_c and \mathbf{x}_d is x_2 . Thus, when \mathbf{x}_c and \mathbf{x}_d are mixed, mask $w_{0111100}$ induces the dependency only between x_2 and x_4 and acts like the mask of size 2. Therefore,

we copy x_2 , then, we copy x_1 and obtain $\mathbf{x}_c' = [0010111] = w_{1100000} + w_{0111100} + w_{0000110} + w_{0000011} = 4$.

To recap, when mixing two individuals, the dependency strength raised by the Walsh coefficient mask depends on the number of differing positions it covers, not on its pure size. For a given pair of individuals, a large mask indicates strong dependencies if the number of differing positions it covers is close or equal to two (lower does not indicate any dependency). Consequently, if a large mask covers many differing positions, its influence on the dependency strength between the covered variables seems less significant.

3.2 Weighted VIG propositions

Using the intuitions explained above, we define the Weighted Dynamic VIG (wdVIG). wdVIG is computed for a given pair of mixed solutions. The value of the wdVIG cell is defined as follows.

$$wdVIG(\mathbf{x}_a, \mathbf{x}_b, g, h) = \frac{\sum_{mask}^{masks(\mathbf{x}_a, \mathbf{x}_b, g, h)} |w_{mask}|}{2 \cdot d(mask, \mathbf{x}_a, \mathbf{x}_b)(d(mask, \mathbf{x}_a, \mathbf{x}_b) - 1)} \quad (1)$$

where \mathbf{x}_a and \mathbf{x}_b are the mixed individuals, g and h are the genes for which we compute the strength of dependency, $masks(\mathbf{x}_a, \mathbf{x}_b, g, h)$ is the set of all non-zero Walsh coefficients, which masks cover x_g and x_h and for which x_g and x_h differ in \mathbf{x}_a and \mathbf{x}_b , $d(mask, \mathbf{x}_a, \mathbf{x}_b)$ is the number of genes differing in \mathbf{x}_a and \mathbf{x}_b covered by the $mask$. Thus, the absolute value of the coefficient is divided by the number of dependencies it raises for a given pair of individuals.

Consider the 4-bit problem, which Walsh decomposition is built from two coefficients: $w_{1110} = w_{0111} = 1$ and two mixed individuals: $\mathbf{x}_e = [0001]$ and $\mathbf{x}_f = [1111]$. In wdVIG, The dependency for x_2 and x_3 will be: $wdVIG(\mathbf{x}_e, \mathbf{x}_f, 2, 3) = |w_{1110}| \cdot \frac{2}{3(3-1)} + |w_{0111}| \cdot \frac{2}{2(2-1)} = \frac{|w_{1110}|}{3} + |w_{0111}|$. Coefficient w_{1110} raises three dependency pairs for \mathbf{x}_e and \mathbf{x}_f , i.e. (1,2), (1,3), and (2,3). Therefore, its influence (the absolute value of the coefficient) is divided by three. Oppositely, for \mathbf{x}_e and \mathbf{x}_f , w_{0111} raises only one dependency pair (2,3) because x_4 is equal \mathbf{x}_e and \mathbf{x}_f .

In wdVIG, the dependency strength depends on the absolute coefficient value and the number of dependencies raised by the coefficient's mask for a given individual pair. To verify wdVIG quality, we will consider three other weighted VIG types.

- (1) wdVIG without mask size influence (wdVIGns) defined as

$$wdVIGns(\mathbf{x}_a, \mathbf{x}_b, g, h) = \sum_{mask}^{masks(\mathbf{x}_a, \mathbf{x}_b, g, h)} |w_{mask}| \quad (2)$$

In wdVIGns, the influence of each coefficient (covering x_g and x_h) equals zero if x_g or x_h are equal in the mixed individuals. Otherwise, it equals the absolute coefficient value.

- (2) weighted static VIG (wsVIG) that equals wdVIG but ignores genotype differences between mixed individuals, defined as

$$wsVIG(g, h) = \sum_{mask}^{masks(g, h)} |w_{mask}| \cdot \frac{2}{size(mask)(size(mask) - 1)} \quad (3)$$

where $masks(g, h)$ is the set of all Walsh coefficients whose masks mark x_g and x_h , and $size(mask)$ is the number of genes marked by the whole mask.

- (3) wsVIG without mask size influence (wsVIGns) considers only the absolute values of all coefficients that mark a given pair of genes. wsVIGns is defined as follows.

$$wsVIGns(g, h) = \sum_{mask \in masks(g, h)} |w_{mask}| \quad (4)$$

We use LTs to cluster the four weighted VIG types proposed above. To show the differences between them, let us consider a 6-bit problem built from four coefficients ($w_{111000} = 10$, $w_{110101} = 8$, $w_{000111} = 7$, and $w_{010100} = 2$). We wish to improve $x_o = [101000]$ by mixing with $x_p = [010110]$. In Table 1, we present all four considered weighted VIG types for x_o and x_p . In Table 2, we present the signs of Walsh coefficients related to x_o and x_p . Table 2 shows that to improve x_o by mixing with x_p , we need to pass the positive sign of w_{110101} and preserve the signs of other coefficients. Thus, we have to copy gene x_4 or genes x_1, x_2 , and x_4 together (because x_6 is the same in x_o and x_p). We do not want to copy x_3 in both cases. Starting from x_4 , we have to copy it with x_2 and x_5 to preserve the signs of w_{010100} and w_{000111} , respectively. If we copy x_2 and x_4 together, then we have to copy x_1 to pass the positive sign of w_{110101} . Thus, we wish to use the following mask $\{1, 2, 4, 5\}$. If we always choose the strongest relation to join LT nodes, then obtaining such a mask for VIGs presented in Tables 1a-1c is impossible because they will first join x_1 and x_2 . We ignore the relation between x_6 and x_4 because x_6 is equal in both individuals. Then, the strongest relation will be between pairs (x_1, x_3) , (x_2, x_3) , and (x_2, x_4) . Thus, x_3 will be added to the node (x_1, x_2) . Such a mask will force passing the sign of w_{111000} from x_p to x_o , which will deteriorate x_o quality.

The situation differs for wdVIG. First, we will join (x_4, x_5) , then (x_1, x_2) and the strongest relation between x_4 and x_2 will join these two nodes into (x_1, x_2, x_4, x_5) , which is the mask we wish to obtain.

3.3 Weighted PX

For problems with high epistasis, PX may become ineffective due to generating masks covering all differences in the mixed individuals (see Section 2.1). Therefore, we propose Weighted PX (wPX), which does not suffer from this disadvantage. In wPX, we use weighted VIG and cluster it using LT. LTs are frequently used as part of OM in SLL-using black-box-dedicated optimizers (see Section 2.2).

When we use SLL in black-box optimization, we do not know which dependencies are direct. Moreover, we do not even know which are true or false. The relation strength for each gene pair is a result of statically-based prediction. Therefore, the strategy to consider all LT nodes (or almost all, since sometimes the nodes with size 1 are ignored) seems justified. However, in gray-box optimization, the situation differs. We know the true dependencies and (at least in the research presented in this work) the Walsh coefficients from which these dependencies arise. Thus, we can choose only those LT nodes that are worth consideration.

In wPX, we assume that we obtain masks from the weighted VIG in which those gene pairs that are the arguments of subfunctions with the highest influence on fitness are highly dependent. Oppositely, the relation strength of those gene pairs that are the

arguments of subfunctions with the low influence on fitness is low. In LT created on the base of such weighted VIG, the nodes on the lowest levels of LT will consist of those variables that are strongly related, while the weakest relations will cause the creation of nodes on top of the tree. If, for a given weighted VIG, a standard PX would create more than one mixing mask, then the same number of disjoint LTs will be created. We propose the following strategy of choosing LT nodes for wPX (denoted as *LTtop*). In *LTtop*, we consider LT roots if more than one LT was created, as well as all nodes that are one level beneath the roots. We ignore all nodes that are full masks (if a single LT was created) and of size 1. Thus, the *LTtop* strategy will limit the number of considered mixing masks, which shall spare the computation resources. At the same time, it will tend to break the weakest relations that caused the creation of nodes right beneath the LT root (for the example, see Section S-V and Fig. S-II, supplementary material).

Similarly to Optimal Mixing employed in P3 and LT-GOMEA [2, 6], in wPX, we try to improve a single individual denoted as *source*. To this end, we randomly choose the *donor* individual, generate weighted VIG for the considered individual pair, obtain LT, and use *LTtop*-selected nodes as mixing masks. If copying genes from the donor to the source individual does not improve the source individual, then the modification to its genotype is rejected. wPX ends if the source individual is improved or none of the considered masks were used.

3.4 Gray-box Optimizer for Problems with High Epistasis

To utilize wPX, we propose Gray-box Optimizer for Problems with High Epistasis (GBO-PHE) that refers to the P3-like population management. GBO-PHE is parameter-less, which seems useful for practical purposes. Its procedure is presented in Pseudocode 1.

Pseudocode 1 The general procedure of GBO-PHE

```

1: Pyramid ← empty;
2: WalshCoeffs ← ComputeWalshCoeffs();
3: while ¬StopCondition do
4:    $x$  ← FIHC(CreateRandomInd());
5:   AddToPyramidLevel(Pyramid, 0,  $x$ );
6:   for each level in Pyramid do
7:     fitnessOld ← Fitness( $x$ );
8:     for each ind in (random order) level do
9:        $x$  ← wPX( $x$ , ind, WalshCoeffs);
10:    if Fitness( $x$ ) > fitnessOld then
11:      AddToPyramidLevel(Pyramid, level + 1,  $x$ );
```

GBO-PHE starts from initializing the pyramid and computing Walsh coefficients (lines 1-2). In each iteration, a new individual x (*climber* in P3) is created randomly, optimized by FIHC (line 4), and added to the lowest level of the pyramid (line 5). Then, x is mixed with the subsequent pyramid levels. While mixed with each level, x acts as the source individual of wPX, while all individuals at a given level are considered in the random order and act as donors (lines 8-9). If mixing with a given level improves the climber's fitness, then its improved copy is added to the next pyramid level (if necessary, a new level is created and initialized with the improved copy of x).

Table 1: Weighted VIGs for a 6-bit problem built from four coefficients ($w_{111000} = 10$, $w_{110101} = 8$, $w_{000111} = 7$, and $w_{010100} = 2$) and individuals $x_o = [101000]$, $x_p = [010110]$.

	1	2	3	4	5	6		1	2	3	4	5	6		1	2	3	4	5	6		1	2	3	4	5	6
1	X	18	10	8	0	8	1	X	4.7	3.3	1.3	0.0	1.3	1	X	18	10	8	0	0	1	X	6.0	3.3	2.7	0.0	0.0
2	18	X	10	10	0	8	2	4.7	X	3.3	3.3	0.0	1.3	2	18	X	10	10	0	0	2	6.0	X	3.3	4.7	0.0	0.0
3	10	10	X	0	0	0	3	3.3	3.3	X	0.0	0.0	0.0	3	10	10	X	0	0	0	3	3.3	3.3	X	0.0	0.0	0.0
4	8	10	0	X	7	15	4	1.3	3.3	0.0	X	2.3	3.7	4	8	10	0	X	7	0	4	2.7	4.7	0.0	X	7.0	0.0
5	0	0	0	7	X	7	5	0.0	0.0	0.0	2.3	X	2.3	5	0	0	0	7	X	0	5	0.0	0.0	0.0	7.0	X	0.0
6	8	8	0	15	7	X	6	1.3	1.3	0.0	3.7	2.3	X	6	0	0	0	0	0	X	6	0.0	0.0	0.0	0.0	0.0	X

(a) wsVIGns

(b) wsVIG

(c) wdVIGns

(d) wdVIG

Table 2: Individuals $x_o = [101000]$, $x_p = [010110]$ and the signs of the Walsh coefficients.

	x_1	x_2	x_3	x_4	x_5	x_6	w_{111000}	w_{110101}	w_{000111}	w_{010100}
x_o	1	0	1	0	0	0	+	-	+	+
x_p	0	1	0	1	1	0	-	+	+	+
diff	1	1	1	1	1	*				
x_r	0	1	1	1	1	0	+	+	+	+

4 Revealing Hidden Problem Structure

In this work, we measure the dependency strength between variables to filter and use only the strongest dependencies that are the most relevant to the optimization process. In this section, we present the results that justify such a choice and aim to answer the following research questions:

RQ1. If we add noise to the problem of a known structure, then how will this influence the Walsh-based problem representation and the VIGs considering non-linear, non-monotonical, and 2DLED dependencies?

RQ2. Can we filter the noise using Walsh coefficients?

RQ3. Can we filter the noise in real-world problems' instances and obtain a strong problem structure for problems that refer to fully connected VIGs?

4.1 Noise modelling and filtering

To investigate the influence of noise on the problem structure, we propose the experiment using the *onemax* problem defined as $onemax(x) = u(x)$, where $u(x)$ is the sum of gene values (*unitation*). We consider 10-bit *onemax* instances. To the value of each problem solution, we add a random real value from the range $(0, nVol)$ where $nVol$ is the maximum noise volume. The problem is *static*, i.e., the noise distorting each solution is chosen once. Thus, each solution always evaluates to the same function value. The considered instances are of toy size because we wish to investigate their complete Walsh representation, i.e., we must compute all Walsh coefficients of all possible sizes. For each problem instance, we construct VIG based on the non-linearity, non-monotonicity, and 2DLED checks. Since the problem instances are of toy size, we perform each check in every available context. In *onemax*, all variables are independent. Thus, all obtained dependencies will originate from noise.

Figure 1a presents *VIG epistasis* (the percentage of non-zero VIG entries) for the three considered dependency types for the noised *onemax* problem. In *onemax*, if two solutions refer to different function values, then the value of this difference is at least one. Thus, for the lowest considered noise, i.e., $nVol = 1$, for any pair of solutions x_a and x_b such that $f(x_a) < f(x_b)$ it is true that $f'(x_a) < f'(x_b)$,

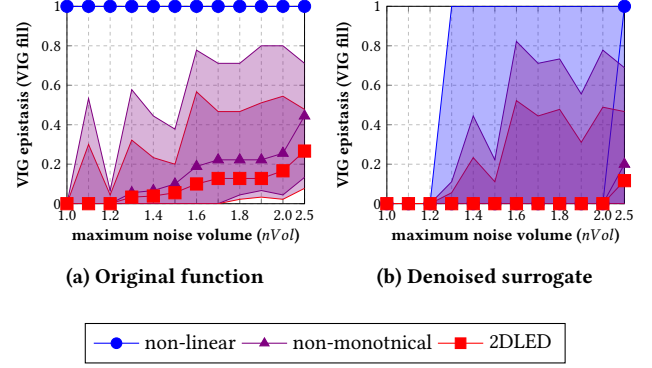


Figure 1: The influence of noise volume on the VIG epistasis for various dependency checks (onemax problem). Lines with markers refer to the median. The bottom and upper lines of the same color refer to maximal and minimal values.

where $f'(x)$ is the original function after adding noise. As presented in Figure 1a, the non-linear VIG becomes a full graph in all tested cases, even for the lowest noise values. Since *onemax* does not yield any dependencies, all discovered dependencies arise from noise and may be considered false. Using such dependencies may deteriorate the effectiveness of the optimizers using it [13].

For DLED and 2DLED VIGs, even their maximal values for the highest noise ($nVol = 2.5$) are not full graphs, and the median epistasis is below 50% and 30%, respectively. This indicates that DLED and 2DLED may be useful in decomposing problem instances in which the optimized function has noise-like characteristics.

Pseudocode 2 Walsh denoise procedure

```

1: function LANDVIS(WalshCoeffsAll)
2:   CoeffsSorted  $\leftarrow$  SortByAbsValueAsc(WalshCoeffsAll);
3:   CoeffsSurr  $\leftarrow$  CoeffsSorted;
4:   OrigOptima  $\leftarrow$  GetAllOptima(CoeffsSorted);
5:   SurrOptima  $\leftarrow$  GetAllOptima(CoeffsSurr);
6:   while OrigOptima = SurrOptima do
7:     CoeffsSurrTry  $\leftarrow$  CoeffsSurr - CoeffsSurr[0];
8:     SurrOptima  $\leftarrow$  GetAllOptima(CoeffsSurrTry);
9:     if OrigOptima = SurrOptima then
10:      CoeffsSurr  $\leftarrow$  CoeffsSurrTry;
return CoeffsSurr;

```

To show that the Walsh function representation may be useful for removing the noise, we propose the *Walsh-based denoise procedure* (Pseudocode 2) dedicated to analyzing toy-sized instances to understand their features. The use of knowledge gathered in this way will be the subject of future work. Considering their absolute value, we sort all Walsh coefficients in increasing order (line 2). We remove subsequent coefficients from the function representation (line 7) as long as, after removing a given coefficient, the global optima of the surrogate are the same as the global optima of the original function (lines 6 and 9). Function representation obtained in this way will be denoted as *denoised surrogate* or *denoised function*.

As presented in Figure 1b, the VIG epistasis of the denoised surrogate is significantly lower for all considered dependency types. For $nVol \leq 1.2$, median epistasis is zero, although in some runs, it may raise to 100% for $nVol \geq 1.3$ and non-linear VIG. Even for the highest considered noise, the epistasis of the denoised surrogate remains low for DLED and 2DLED VIGs.

Table 3: The influence of the mask size and noise volume on the median minimum absolute Walsh coefficient value.

noise volume ($nVol$)	Walsh coefficient mask size			
	2	3	4	5
1.0	2.0E-4	4.2E-5	1.1E-7	1.5E-7
1.1	1.5E-4	4.5E-7	7.0E-8	7.0E-8
1.2	2.1E-4	4.3E-5	8.5E-8	3.0E-8
1.3	3.6E-4	2.4E-5	8.0E-8	8.0E-8
1.4	3.3E-4	8.6E-7	1.3E-7	1.3E-7
1.5	3.1E-4	2.7E-5	1.1E-7	6.5E-8
1.6	2.9E-4	6.5E-7	2.2E-7	7.5E-8
1.7	3.4E-4	3.9E-5	1.5E-7	1.0E-7
1.8	2.7E-4	7.9E-5	1.9E-7	5.0E-8
1.9	3.7E-4	5.8E-5	1.7E-7	6.0E-8
2.0	5.7E-4	1.1E-4	1.2E-7	3.6E-7
2.5	4.4E-4	8.5E-5	1.5E-7	2.2E-7

In onemax, all Walsh coefficients with masks of size 2 or higher are zero. Thus, analyzing such coefficients for the noised onemax will show how the noise may influence those absolute coefficient values that refer to variable dependencies. The median and maximum values were similar for all mask sizes. Therefore, in Table 3, we report the median of the minimal absolute Walsh coefficient values for masks of a given size. This value is significantly higher for Walsh coefficients referring to masks of size two. Thus, the denoise procedure will consider many Walsh coefficients with longer masks first. This indicates that the noise modelled by Walsh coefficients with masks of size two may be relatively hard to remove. Such observations are coherent with the research presented in [25].

The results reported in this section indicate that the dependency checks based on non-monotonicity are more useful than the non-linearity check for decomposing problems with noise-like features. The proposed denoised procedure may be useful in limiting the number of dependencies caused by noise for sufficiently short problem instances. Finally, we show that Walsh coefficients referring to the masks of size 2, that model the noise may be the hardest to remove using the proposed denoised procedure.

4.2 Denoising real-world instances

We consider two real-world feature selection problems, Bare Soil Detection in Remotely-sensed Earth Observation data [9, 20] and Anomaly Detection in Satellite Telemetry [18]. Section S-I (supplementary material) highlights their importance and details. In both

cases, compressing machine learning pipelines—by selecting discriminative features or optimizing models—is essential for practical deployment. Without such optimization, the models may become unusable, as they cannot be onboarded to the target environment.

We divide the problems tackled in our experimental study into three groups: kNN, BS (bare soil detection), and OPS (OPS-SAT telemetry analysis). Note that each of these groups considers many different quality measures. Thus, these are groups of different problems. Nevertheless, for presentation clarity, we will show the summarized results divided into these three groups.

Table 4: VIG epistasis of the considered real-world instances for various dependency checks after denoising procedure.

	non-linearity			non-monotonicity			2DLED		
	kNN	BS	OPS	kNN	BS	OPS	kNN	BS	OPS
min	0.00	1.00	0.27	0.00	0.42	0.05	0.00	0.38	0.03
max	1.00	1.00	1.00	0.95	0.82	0.90	0.71	0.60	0.70
avr	1.00	1.00	0.90	0.42	0.53	0.48	0.25	0.47	0.30
std	0.05	0.00	0.22	0.19	0.09	0.22	0.13	0.04	0.18
med	1.00	1.00	1.00	0.37	0.51	0.46	0.22	0.47	0.25

For every considered real-world problem instance, all considered VIG types were full graphs. However, VIGs obtained after denoising differ significantly. Table 4 shows that for the denoised surrogate, the non-linear VIG may be an empty graph (no dependent variable pairs). Nevertheless, most non-linear VIGs remain a full graph. Similarly to results presented for noised onemax, non-monotonicity check and 2DLED seem to be more useful, i.e., the VIG epistasis for these dependency types is significantly lower and does not reach 100% in any of the performed runs.

Table 5: The number of maximum full subgraphs for VIGs concerning various dependency checks for considered real-world instances.

	non-linearity		non-monotonicity		2DLED	
	Number*	Len**	Number	Len	Number	Len
kNN	1 1/15	1/15	15 5/36	1/12	27 13/180	1/12
BS	1 1/1	19/19	9 3/142	1/14	13 6/383	1/14
OPS	1 1/23	1/18	25 9/46	1/13	58 21/239	1/13

* statistics in Number column: med min/max

** statistics in Len column: min/max

In Table 5, we present the number of maximal full subgraphs (cliques) obtained for VIGs of various types constructed for denoised surrogates. Maximal full subgraphs of a VIG can be interpreted as sets of entry variables to subfunctions in the additive form [1]. Thus, if the problem has a strong structure it should decompose into many subfunctions (overlapping or not). Table 5 shows that for the non-linear VIG, the median number of maximal full subgraphs is 1 (because the median epistasis of non-linear VIG is 100%). However, even for non-linear VIG, in some cases, the number of maximal full subgraphs is equal to the number of function arguments, which shows that after denoising, we deal with a fully separable problem in which each variable can be optimized separately.

For non-monotonicity and 2DLED VIGs, the number of maximal full subgraphs is high. It sometimes exceeds the number of function variables, which shows that the denoised problem is built from overlapping subfunctions. Finally, for these VIGs, the lowest number of maximal full subgraphs is always higher than one. Thus, we

can state that all of the considered instances have a decomposable structure hidden under the noise.

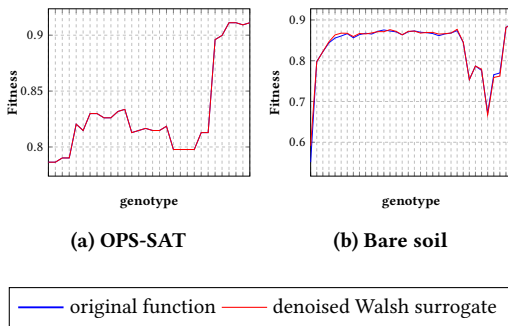


Figure 2: A landscape cross-section for chosen problem instances (solution opposite to global optimum \rightarrow global minimum \rightarrow global maximum; differing genes are modified in a random order). See Fig. S-1, supplementary material, for more results.

[ht]

To compare the landscapes of the original and denoised function we construct graphs in the following manner (for details, see Section S-III and Pseudocode S-1, supplementary material). We randomly choose one of the global optima and one of the global minima. We start from the solution opposite to the chosen global optimum, *move* to the chosen global minimum, and *move* to the chosen global maximum. By *moving*, we consider flipping the genes differing in start and destination solutions. Figure 2 shows two representative curves. All curves for the original function have the same shape as the curves obtained for the denoised surrogates.

The results presented in this section lead to the following conclusions. Adding the noise to the optimized function may cause its VIG to become a full graph. VIGs based on the non-monotonicity check and 2DLED are significantly less vulnerable to discovering the dependencies caused by noise. The denoised surrogates of all the considered real-world instances are characterized by strong structure, even though for their original forms, we obtain full graphs for all considered VIG types. Thus, using weighted VIGs to identify and eliminate at least some part of the weakest dependencies is promising.

5 Main Experiments

5.1 Experiment setup and considered optimizers

To verify the quality of the proposed wPX, we consider a set of benchmarks typical for the GA-related research, which includes the concatenations of: standard deceptive functions of order 8 [4] (denoted as *dec8*), bimodal deceptive functions of order 6 and 10 [5] (*bim6* and *bim10*). We also consider the cyclic traps built from these functions with various overlap size (e.g., *dec8* with 5 overlapping genes for both neighbouring functions is denoted as *dec8o5*). Finally, the set of problems was supplemented by NK-fitness landscapes of $k = 6$ [6] (*nkLand6k*), and Ising Spin Glasses [6, 19] (*ISG*). The detailed definitions of these problems can be found in the supplementary material in Section S-IV.

All problems were considered in their standard and noised versions. The results presented in Section 4.1 show that the noised-caused Walsh coefficients with masks of size 2 are the hardest to remove because their minimal absolute value is significantly higher than the minimal absolute value of coefficients with larger masks. Here, we consider problem instances that can be considered as large. Thus, adding random noise to each solution in the manner employed in Section 4.1 is impossible. To simulate the noise, we randomly add the Walsh coefficient with a mask of size 2 for each variable, joining it with a randomly chosen variable. The absolute value of such a coefficient is small enough not to change the majority/minority relation between the fitness of any two solutions. However, two solutions with equal fitness in the original function can become unequal after adding noise. We consider adding 0, 1, 2, 3, 4, and 5 randomly generated Walsh coefficients of size 2 per a single variable (adding 0 coefficients refers to the original function).

In Section 3.4, we propose GBO-PHE using wPX that employs wdVIG and the LTop strategy. To justify the intuitions behind these choices, we also consider GBO-PHE using *LBot* strategy (denoted as *GBO-PHE-LBot*) that considers all LT nodes in the P3 manner (the shorter nodes go first, the order of the nodes of the same size is random). Additionally, we consider other weighted VIG versions considered in this work, i.e., wdVIGs, wsVIG, and wsVIGns. Finally, the competing optimizer set is supplemented by GBO-PHE using standard PX (*GBO-PHE-PX*). The considered optimizer set was supplemented by P3 and LT-GOMEA, which are black-box optimizers. To make the comparison fair, they were supported a VIG and did not use any problem decomposition mechanisms.

All the considered optimizers are parameter-less and no tuning was necessary. The computation budget was set to $2 \cdot 10^6$ fitness function evaluations (FFE). The gray-box settings refer only to access to Walsh-based function representation, no partial evaluations were used. Each experiment was repeated 30 times. The source code of all optimizers was joined in one C++ project and is available on Zenodo [12] and GitHub¹ (with the results and setting files).

5.2 Results

In Table 6, we present the general comparison of the considered optimizers. For each problem, we report the largest problem size for which a given optimizer has an optimal solution in at least 80% of the runs. If two optimizers are successful for the same problem's size, we consider such a result as a tie. We avoid further comparing which of them obtained a given result faster (in terms of FFE) because the differences seem negligible, and even if statistically significant, they would not show true supremacy.

As presented, GBO-PHE-LTop-wdVIG was the most effective optimizer. It was outperformed only for *bim10*. For all the other problems, it was able to optimize the largest problem instances, regardless of whether they were noised or not. The effectiveness of GBO-PHE-LBot-wdVIG was worse because this GBO-PHE version considers a higher number of masks, which, for some problems, was too expensive. The effectiveness of GBO-PHE-LTop-wdVIGns was the same as GBO-PHE-LBot-wdVIG for many problems. Such results show that dynamically adjusting the considered Walsh Coefficients and using the LTop strategy was more significant than

¹<https://github.com/przewooz/wVIG>

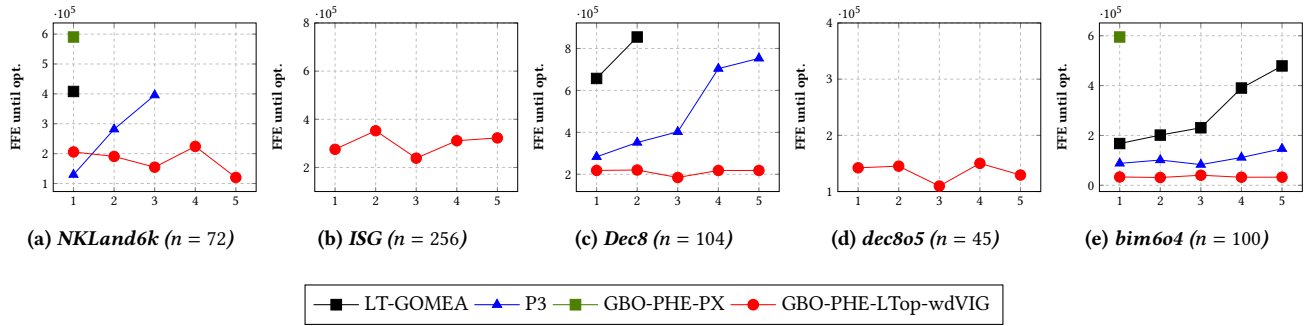


Figure 3: Scalability for chosen instances and increasing noise (X axis: number of random Walsh coefficients per variable).

Table 6: Maximum problem size for which a given optimizer found an optimal solution in at least 80% of the runs. GBO-PHE-LTop-wdVIG was the most effective. Therefore, we compare all other optimizers with this version of GBO-PHE.

	noise	GBO-PHE											
		P3	LT-GOMEA	stand PX	Top wdVIG	Bottom wdVIG	Top wsVIG	Bottom wsVIG	Top wdVIGns	Bottom wdVIGns	Top wsVIGns	Bottom wsVIGns	
nkLand6k	0	102	72	204	204	150	48	24	150	150	24	48	
nkLand6k	5	48	48	24	150	150	24	48	150	102	24	48	
ISG	0	N/A	N/A	625	784	256	N/A	N/A	784	256	N/A	N/A	
ISG	5	N/A	N/A	N/A	400	256	N/A	N/A	400	256	N/A	N/A	
bim6	0	204	204	204	204	204	204	204	204	204	204	204	
bim6	5	204	204	30	204	204	12	204	204	204	12	204	
bim10	0	60	100	60	50	50	30	30	30	20	20	30	
bim10	5	30	50	N/A	50	20	20	N/A	30	20	20	N/A	
bim6o4	0	200	200	200	200	200	16	200	200	200	16	200	
bim6o4	5	200	150	30	200	200	16	200	200	200	16	200	
dec8	0	200	152	200	200	152	200	152	200	152	200	104	
dec8	5	104	16	16	152	152	16	104	152	152	16	104	
dec8o5	0	15	15	60	60	15	15	15	60	15	15	15	
dec8o5	5	15	15	15	60	15	15	15	60	15	15	15	
better than GBO-PHE-LTop-wdVIG		1	1	1	N/A	0	0	0	0	0	0	0	
worse than GBO-PHE-LTop-wdVIG		8	9	8	N/A	7	12	10	3	10	12	10	

considering the mask size influence. Nevertheless, this latter mechanism also positively influences the quality of the results.

The comparison with P3, LT-GOMEA, and GBO-PHE using standard PX was decisive. These optimizers can not effectively handle problems with noise because they are using too large masks. For some problems (e.g., dec8o5), the considered gray-box versions of P3 and LT-GOMEA performed worse than expected. This situation is because their black-box versions discover dependencies and create different LTs during the run. Here, they were using true but static VIG, which deteriorated their effectiveness in some cases. Such a result is justified because when solving overlapping problems, using many diverse LTs is beneficial for these optimizers [15].

The above observations are confirmed by the scalability analysis presented in Fig. 3. Note that the influence of increasing noise is negligible for GBO-PHE-LTop-wdVIG. At the same time, the effectiveness of the traditional optimizers deteriorates significantly.

6 Conclusions

In this work, we propose and verify experimentally various weighted VIGs created on the base of Walsh coefficients. Proposed mechanisms allow the effective optimization of problems with and without noise. However, the proposed ideas and their experimental verifications may have a broader meaning. Since we model the noise by adding random-based Walsh coefficients to the problem definition, we can generate instances with the increasing influence of noise and verify which mechanisms remain effective in such scenarios. The

proposed wdVIG extends the idea of using Walsh decomposition to construct VIG without deteriorating existing VIG advantages. For problems without noise, wdVIG is equivalent to VIG, but for noised problems, its advantage over traditional VIG is significant.

The proposed experiments show that for real-world problem instances that are currently considered to have a weak problem structure, there is a potential to propose a mechanism that can uncover their strong structure. Here, we only show the existence of a strong structure in the toy-sized problem instances. However, proposing denoising mechanisms for large-scale instances is the most important direction for future work. It can enable using gray-box operators such as PX for problems they currently do not apply.

Acknowledgments

We want to thank Darrell Whitley for the valuable discussions on Walsh decomposition, which were one of the inspirations for writing this work.

The work was supported by: Polish National Science Centre (NCN), Grant 2022/45/B/ST6/04150 (Michal Przewozniczek); University of Malaga, project PAR 4/2023 (Francisco Chicano); National Council for Scientific and Technological Development, CNPq grant #306689/ 2021-9 and FAPESP grant #2024/15430-5 (Renato Tinós); European Space Agency (ESA), projects 40001373339/22/NL/GLC/ov and 4000141301; FESL.10.25-IZ.01-07G5/23 (Agata Wijata); Silesian University of Technology (Jakub Nalepa); Opole University of Technology, DELTA project no. 272/24 (Bogdan Ruszczak).

References

- [1] Georgios Andreadis, Tanja Alderliesten, and Peter A. N. Bosman. 2024. Fitness-based Linkage Learning and Maximum-Clique Conditional Linkage Modelling for Gray-box Optimization with RV-GOMEA. In *Proceedings of the Genetic and Evolutionary Computation Conference (Melbourne, VIC, Australia) (GECCO '24)*. Association for Computing Machinery, New York, NY, USA, 647–655. doi:10.1145/3638529.3654103
- [2] Peter A.N. Bosman, Ngoc Hoang Luong, and Dirk Thierens. 2016. Expanding from Discrete Cartesian to Permutation Gene-pool Optimal Mixing Evolutionary Algorithms. In *Proceedings of the Genetic and Evolutionary Computation Conference 2016 (GECCO '16)*. ACM, 637–644.
- [3] Francisco Chicano, Darrell Whitley, Gabriela Ochoa, and Renato Tinós. 2024. Generalizing and Unifying Gray-Box Combinatorial Optimization Operators. In *Parallel Problem Solving from Nature – PPSN XVIII: 18th International Conference, PPSN 2024, Hagenberg, Austria, September 14–18, 2024, Proceedings, Part I (Hagenberg, Austria)*. Springer-Verlag, 52–67.
- [4] Kalyanmoy Deb and David E. Goldberg. 1993. Sufficient Conditions for Deceptive and Easy Binary Functions. *Ann. Math. Artif. Intell.* 10, 4 (1993), 385–408.
- [5] Kalyanmoy Deb, Jeffrey Horn, and David E. Goldberg. 1993. Multimodal Deceptive Functions. *Complex Systems* 7, 2 (1993).
- [6] Brian W. Goldman and William F. Punch. 2014. Parameter-less Population Pyramid. In *Proceedings of the 2014 Annual Conference on Genetic and Evolutionary Computation (Vancouver, BC, Canada) (GECCO '14)*. ACM, 785–792.
- [7] R. B. Heckendorn. 2002. Embedded Landscapes. *Evolutionary Computation* 10, 4 (2002), 345–369.
- [8] Shih-Huan Hsu and Tian-Li Yu. 2015. Optimization by Pairwise Linkage Detection, Incremental Linkage Set, and Restricted / Back Mixing: DSMGA-II. In *Proceedings of the 2015 Annual Conference on Genetic and Evolutionary Computation (GECCO '15)*. ACM, 519–526.
- [9] Israr Majeed, Naveen K. Purushothaman, Poulamee Chakraborty, et al. 2023. Estimation of soil and crop residue parameters using AVIRIS-NG hyperspectral data. *International Journal of Remote Sensing* 44, 6 (2023), 2005–2038. doi:10.1080/01431161.2023.2195570
- [10] M. Munetomo and D.E. Goldberg. 1999. A genetic algorithm using linkage identification by nonlinearity check. In *IEEE SMC'99 Conference Proceedings. 1999 IEEE International Conference on Systems, Man, and Cybernetics (Cat. No.99CH37028)*, Vol. 1. 595–600 vol.1. doi:10.1109/ICSMC.1999.814159
- [11] Masaharu Munetomo and David E. Goldberg. 1999. Linkage identification by non-monotonicity detection for overlapping functions. *Evol. Comput.* 7, 4 (dec 1999), 377–398. doi:10.1162/evco.1999.7.4.377
- [12] Michal Witold Przewozniczek, Francisco Chicano, Renato Tinós, Jakub Nalepa, Bogdan Ruzszczak, and Agata Wijata. 2025. Replication package of the publication “On Revealing the Hidden Problem Structure in Real-World and Theoretical Problems Using Walsh Coefficient Influence”. Zenodo. doi:doi.org/10.5281/zenodo.15179339
- [13] Michal W. Przewozniczek, Bartosz Frej, and Marcin M. Komarnicki. 2020. On Measuring and Improving the Quality of Linkage Learning in Modern Evolutionary Algorithms Applied to Solve Partially Additively Separable Problems. In *Proceedings of the 2020 Genetic and Evolutionary Computation Conference (Cancun, Mexico) (GECCO '20)*. Association for Computing Machinery, New York, NY, USA, 742–750.
- [14] Michal Witold Przewozniczek, Bartosz Frej, and Marcin Michal Komarnicki. 2025. From Direct to Directional Variable Dependencies—Nonsymmetrical Dependencies Discovery in Real-World and Theoretical Problems. *IEEE Transactions on Evolutionary Computation* 29, 2 (2025), 490–504. doi:10.1109/TEVC.2024.3496193
- [15] Michal W. Przewozniczek and Marcin M. Komarnicki. 2020. Empirical Linkage Learning. *IEEE Transactions on Evolutionary Computation* 24, 6 (Dec 2020), 1097–1111.
- [16] Michal W. Przewozniczek, Renato Tinós, Bartosz Frej, and Marcin M. Komarnicki. 2022. On Turning Black - into Dark Gray-Optimization with the Direct Empirical Linkage Discovery and Partition Crossover. In *Proceedings of the Genetic and Evolutionary Computation Conference (Boston, Massachusetts) (GECCO '22)*. Association for Computing Machinery, New York, NY, USA, 269–277. doi:10.1145/3512290.3528734
- [17] Michal Witold Przewozniczek, Renato Tinós, and Marcin Michal Komarnicki. 2023. First Improvement Hill Climber with Linkage Learning – on Introducing Dark Gray-Box Optimization into Statistical Linkage Learning Genetic Algorithms. In *Proceedings of the Genetic and Evolutionary Computation Conference (Lisbon, Portugal) (GECCO '23)*. ACM, 946–954.
- [18] Bogdan Ruzszczak, Krzysztof Kotowski, David Evans, and Jakub Nalepa. 2024. The OPS-SAT benchmark for detecting anomalies in satellite telemetry. arXiv:2407.04730 [eess.SP] <https://arxiv.org/abs/2407.04730>
- [19] Lawrence Saul and Mehran Kardar. 1994. The 2D±J Ising spin glass: exact partition functions in polynomial time. *Nuclear Physics B* 432, 3 (1994), 641–667.
- [20] Nélida Elizabet Quiñonez Silvero et al. 2021. Soil variability and quantification based on Sentinel-2 and Landsat-8 bare soil images: A comparison. *Remote Sens. Environ.* 252 (2021). doi:10.1016/j.rse.2020.112117
- [21] Dirk Thierens and Peter A.N. Bosman. 2013. Hierarchical Problem Solving with the Linkage Tree Genetic Algorithm. In *Proceedings of the 15th Annual Conference on Genetic and Evolutionary Computation (GECCO '13)*. ACM, 877–884.
- [22] Renato Tinós, Michal Przewozniczek, Darrell Whitley, and Francisco Chicano. 2023. Genetic Algorithm with Linkage Learning. In *Proceedings of the Genetic and Evolutionary Computation Conference (Lisbon, Portugal) (GECCO '23)*. Association for Computing Machinery, New York, NY, USA, 981–989. doi:10.1145/3583131.3590349
- [23] Renato Tinós, Michal W. Przewozniczek, and Darrell Whitley. 2022. Iterated Local Search with Perturbation Based on Variables Interaction for Pseudo-Boolean Optimization. In *Proceedings of the Genetic and Evolutionary Computation Conference (Boston, Massachusetts) (GECCO '22)*. ACM, 296–304.
- [24] Renato Tinós, Darrell Whitley, and Francisco Chicano. 2015. Partition Crossover for Pseudo-Boolean Optimization. In *Proceedings of the 2015 ACM Conference on Foundations of Genetic Algorithms XIII (Aberystwyth, United Kingdom) (FOGA '15)*. Association for Computing Machinery, New York, NY, USA, 137–149. doi:10.1145/2725494.2725497
- [25] Sébastien Verel, Bilel Derbel, Arnaud Liefvooghe, Hernán Aguirre, and Kiyoshi Tanaka. 2018. A Surrogate Model Based on Walsh Decomposition for Pseudo-Boolean Functions. In *Parallel Problem Solving from Nature – PPSN XV*, Anne Auger, Carlos M. Fonseca, Nuno Lourenço, Penousal Machado, Luís Paquete, and Darrell Whitley (Eds.). Springer International Publishing, Cham, 181–193.
- [26] D. Whitley. 2019. Next generation genetic algorithms: a user's guide and tutorial. In *Handbook of Metaheuristics*. Springer, 245–274.
- [27] Darrell Whitley, Hernan Aguirre, and Andrew Sutton. 2020. Understanding Transforms of Pseudo-Boolean Functions. In *Proceedings of the 2020 Genetic and Evolutionary Computation Conference (Cancun, Mexico) (GECCO '20)*. Association for Computing Machinery, New York, NY, USA, 760–768.
- [28] L. Darrell Whitley, Francisco Chicano, and Brian W. Goldman. 2016. Gray Box Optimization for Mk Landscapes Nk Landscapes and Max-Ksat. *Evol. Comput.* 24, 3 (Sept. 2016), 491–519. doi:10.1162/EVCO_a_00184